International Journal of Solids and Structures 51 (2014) 4294–4306

Contents lists available at ScienceDirect

International Journal of Solids and Structures

journal homepage: www.elsevier.com/locate/ijsolstr

Prismatic tensegrity structures with additional cables: Integral symmetric states of self-stress and cable-controlled reconfiguration procedure

Pei Zhang [a,b,*], Ken'ichi Kawaguchi [c,d], Jian Feng [a,b]

[a] School of Civil Engineering, Southeast University, Nanjing 210096, China
[b] National Prestress Engineering Research Center, Southeast University, Nanjing 210096, China
[c] Department of Architecture, The University of Tokyo, Komaba 4-6-1, Meguro-ku, Tokyo 153-8505, Japan
[d] Institute of Industrial Science, The University of Tokyo, Komaba 4-6-1, Meguro-ku, Tokyo 153-8505, Japan

ARTICLE INFO

Article history:
Received 13 October 2013
Received in revised form 28 July 2014
Available online 28 August 2014

Keywords:
Prismatic tensegrities
Integral symmetric prestress
Eigenvalue analysis
Reconfiguration procedure
Tangent stiffness matrix
Moore–Penrose generalized inverse

ABSTRACT

A simple energy method is put forward to determine the prestress distribution for symmetric tensegrity structures with multiple states of self-stress and a class of prismatic tensegrities with additional cables are introduced to show the accuracy of presented method. For the purpose of modifying structural shape as well as mechanical properties, a cable-controlled reconfiguration procedure is subsequently proposed for these structures. By defining the length adjustments as the control parameters, the reconfiguration procedure is regarded as a quasi-static process, consisting of a sequence of equilibrium configurations with varying control parameters. Then the nonlinear iterative algorithm based on the tangent stiffness of the structure is presented to simulate and follow this reconfiguration process. By way of example, a particular class of reconfigurations coined symmetrical reconfigurations are investigated carefully and the key features as well as the potential applications are given.

1. Introduction

In 1947, a young artist named Kenneth Snelson invented and built a novel framework that he called floating compression. Later, Fuller (1962) called Snelson's structure a tensegrity, and since then, this nomenclature has been dominant in the scientific community.

A tensegrity is a lightweight space structure consisting of compression members (called struts) surrounded by a network of tension members (called cables). The rigidity of a tensegrity is the result of a self-stressed equilibrium between cables and struts. Therefore tensegrities need to have special geometrical configurations that lead to, at least, one state of self-stress in the absence of external forces. The representative and well-known examples for them are a set of prismatic ones composed of v struts and $3v$ cables, requiring special twist angles θ between the top and bottom polygons to maintain the self-equilibrium shapes. Depending on the value of v and the offset between vertices connected by strut, θ has been determined through a simple analytical approach (Connelly and Terrell, 1995) as

$$\theta = 180^\circ \cdot \left(\frac{1}{2} - \frac{j}{v}\right) \tag{1}$$

where j is an integer smaller than v and represents the offset between vertices connected by strut. The top views of some classic prismatic tensegrities as well as the corresponding twist angles are shown in Fig. 1.

These structures are excellent samples with single state of self-stress, whose initial prestress distribution can be determined easily through the linear-algebraic treatment of equilibrium matrix (Pellegrino, 1993; Pellegrino and Calladine, 1986). However, for tensegrity structures with multiple states of self-stress, the further work of finding a suitable linear combination of independent states of self-stress need to be performed (hence the term force-finding or force-design sometimes used). In most of the existing methods, the shape and member forces of tensegrity structures are to be determined simultaneously in order to discover novel shapes, which is called form-finding (the recent review related to this topic can be found in Tibert and Pellegrino, 2011 and Juan and Mirats Tur, 2008). However, so far only a few studies have been carried out to determine the prestress distribution for a given structure with multiple states of self-stress.

* Corresponding author at: School of Civil Engineering, Southeast University, Nanjing 210096, China.

http://dx.doi.org/10.1016/j.ijsolstr.2014.08.014
0020-7683/

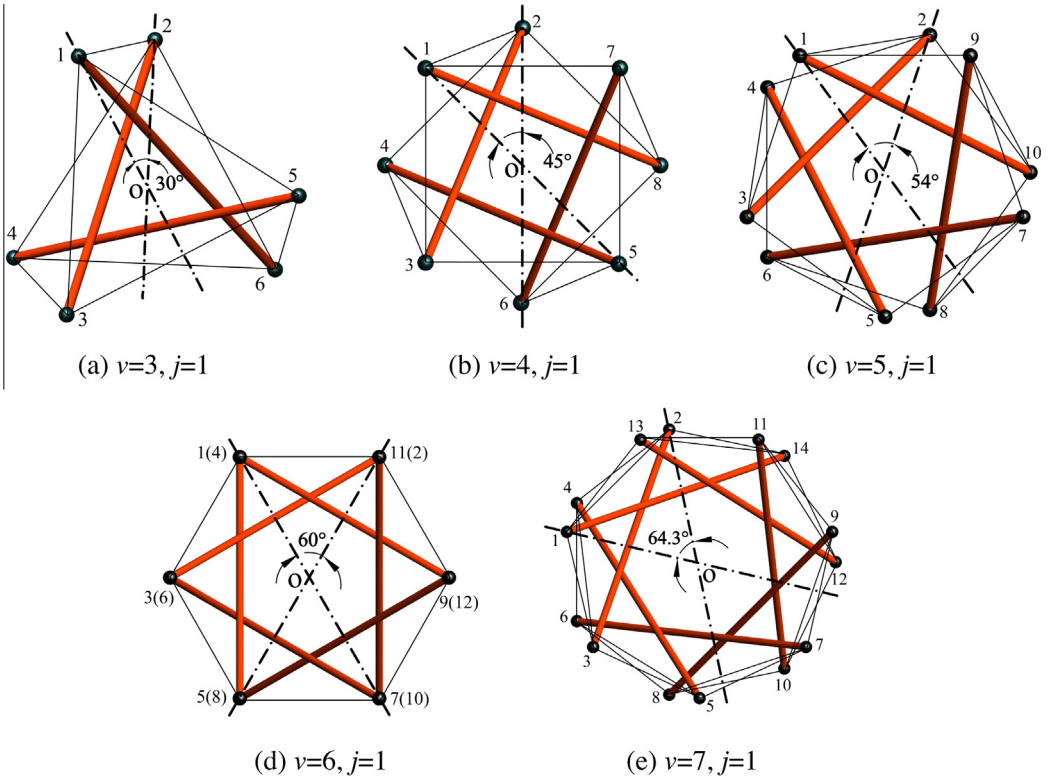

Fig. 1. Top views of some classic prismatic tensegrities.

In practical situations, tensegrity structures usually have symmetric properties, i.e. invariance conditions by reflection with respect to some planes and/or rotation around some axes, which should be taken into account for the determination of prestress distribution. Connelly and Back (1998) have previously considered the effect of symmetry on equilibrium relationships, in which the equilibrium only needs to be checked for one reference node of each "orbit" (symmetrically located nodes are said to belong to the same orbit). Sultan et al. (2001) derived the general prestressability conditions for tensegrity structures from the principle of virtual work and gave the analytical solutions including the state of self-stress for particular classes of symmetrical prestressable configurations. Kangwai and Guest (2000), Zhang et al. (2009) and Chen and Feng (2012) employed group representation theory to block-diagonalise the equilibrium matrix of a symmetric structure. Then the work done on the linear-algebraic analysis of equilibrium matrix, e.g. Calladine (1978), Pellegrino and Calladine (1986), Pellegrino (1993) is equally applicable to these submatrix blocks to gain the symmetric states of self-stress. Although this method can be extended to the structures with any type of symmetry systematically, it has been described in the terminologies of mathematics based on group representation theory and a more comprehensible approach might be favorable to engineering researchers. Hence a practical method based on the group division of members was presented by Yuan and Dong (2003). In that paper, the symmetrically located members were packed into same groups and the constraint that all members in each group have the same stress was imposed on the general expression of self-stress states. A discussion on proper division of member groups for the purpose of existence of the single symmetric state of self-stress has been explicitly given in Tran and Lee (2010). Most recent study employing grouping scheme in force-finding of tensegrity structures can be found in Lee et al. (2014) where a genetic algorithm was also used. However, because the member groups are directly assigned by designers in terms of geometric symmetry of the structure, this approach would suffer from difficulties or make mistakes when applied to, for example, the structures where the topological relationships of members are complicated and the symmetric properties cannot be observed readily.

In the first part of this article, a simple energy method making use of eigenvalue analysis is proposed to determine the prestress distribution for symmetric tensegrity structures with multiple states of self-stress. Essentially, it is to achieve a special orthonormal basis spanning the space of integral symmetric states of self-stress, which satisfy the stationary condition of initial strain energy simultaneously. Since the effect of symmetry is not considered directly in this method, certain symmetry-related operations performed in previous works, e.g. grouping members are avoided. Thus it is more convenient to treat the structures with large number of members and complicated topology. By way of example, a class of prismatic tensegrities with additional cables, which are the variations on the classic ones shown in Fig. 1, are introduced to show the validity and accuracy of the presented method.

On the other hand, as flexible structures, tensegrities are capable of large displacement so that they provide innovative possibilities for physically integrated structure and controller design. Moreover, the control systems can be easily embedded in the structures since the elastic components can carry both sensing and actuating functions. Early work on this topic has been performed by Djouadi et al. (1998) to control the vibrations of a cantilever beam formed by four tensegrities modules. Sultan et al. (2000) formulated control techniques and illustrated it with the example of an aircraft motion simulator. Skelton et al. (2001) developed an explicit analytical model of nonlinear dynamics for shape control of a shell class of tensegrity structures. Fest et al. (2003, 2004) focused on maintaining serviceability through active control and tested a full-scale prototype of an adjustable tensegrity. Sultan et al. (2002) controlled the height of the upper level

under loading using symmetrical motion based on Lagrangian dynamics. Controlling larger movements in tensegrity structures also provided interesting perspectives in the field of deployable structures (Sultan and Skelton, 2003).

In the second part of this article, based on the structures introduced in the first part, a cable-controlled reconfiguration procedure is put forward, in which only added cables are assumed to be adjustable and provide the driving force to change the shape as well as mechanical properties of the structures. By defining the length adjustments as the control parameters, this reconfiguration procedure is regarded as a quasi-static process, consisting of a sequence of equilibrium configurations with varying control parameters. In order to determine these configurations (i.e. simulate and follow this reconfiguration process), a governing equation relating nodal displacements and imposed length change of members is derived and the corresponding nonlinear iterative program based on Newton–Raphson method is also developed. Moreover, the Moore–Penrose generalized inverse of tangent stiffness matrix is used within each corrective iteration to treat the situation that the structure is free-standing. From a practical perspective, a particular class of reconfigurations coined symmetrical reconfigurations are investigated carefully combining with numerical examples and the key features as well as the potential application are also given.

2. Integral symmetric states of self-stress

2.1. Definition for a class of prismatic tensegrity structures with specific additional cables

In this section, a class of prismatic tensegrities are designed, which are the variations on the classic ones shown in Fig. 1. To guarantee the existence of multiple states of self-stress, v vertical cables have been added to connect certain pairs of nodes so that these structures consists of $2v$ nodes and $5v$ members, made up of $4v$ cables and v struts. The nodes are arranged in two horizontal circles of radius R around the vertical z-axis. Within each circle, each node is connected by horizontal cables to two adjacent nodes. The two planes containing the nodes are at $z = 0$ and $z = H$ respectively, where H is the height of structures. Each node in top circle is not only connected by a vertical cable to the corresponding node in bottom circle, but also connected by an additional cable to the adjacent node in bottom circle. Each node in bottom circle is connected by a strut to the adjacent node in top circle, i.e., correspond to the case of $j = 1$ in Eq. (1). A graphical illustration for the topology rule of member connection is shown in Fig. 2.

For the sake of clarity, Fig. 3 shows the triangular and quadrangular prismatic tensegrities with specific additional cables described above, where the added cables are denoted by dot lines. Certainly, other cases with different arrangement of added cables also can be analyzed by the following scheme similarly if necessary.

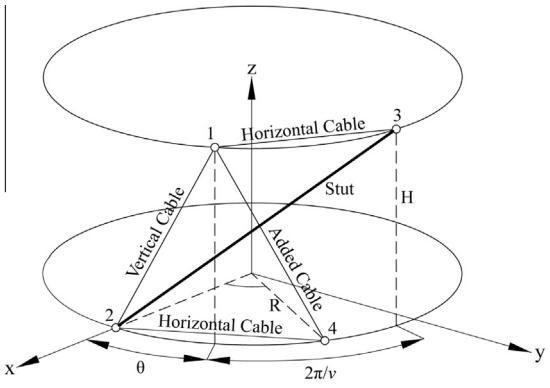

Fig. 2. Connectivity of members.

Consider this type of tensegrity structures floating in three-dimensional space without any kinematic constraints. The self-equilibrium equations at nodes can be written in the form (see Pellegrino and Calladine, 1986)

$$\mathbf{An} = 0 \tag{2}$$

where $\mathbf{A}$ is the equilibrium matrix of the structure containing the orientations of members, $\mathbf{n}$ is the vector consists of the tension in each member. Its right-hand side is equal to a zero vector, since this equation describes equilibrium of nodes without any external loads. Then the number of independent states of self-stress s and internal inextensional mechanisms m can be calculated by following equations, as described in calladine, 1978 and Pellegrino and Calladine, 1986, etc

$$s = 5v - r \quad \& \quad m = 3 \cdot (2v) - r - 6 \tag{3}$$

where r is the rank of $\mathbf{A}$. We compare the calculation results of s and m between the structures with added cables and the corresponding classic ones (up to 7 struts). It can be seen from Table 1 that the addition of v cables add to the states of self-stress to give $s = 3$ in each case, i.e., the existence of multiple states of self-stress is guaranteed for this class of tensegrity structures.

Actually, the Nullspace of $\mathbf{A}$ is precisely the space of self-stress states (i.e. represents all states of self-stress of the assembly), an orthonormal basis of which can be computed by using singular value decomposition for $\mathbf{A}$ (Pellegrino, 1993). Thus a general self-stress state $\mathbf{n}$ can be written as follows by any linear combination.

$$\mathbf{n} = \mathbf{s}_1\alpha_1 + \mathbf{s}_2\alpha_2 + \cdots + \mathbf{S}_s\alpha_s = \mathbf{S}\boldsymbol{\alpha} \tag{4}$$

where $\mathbf{s}_i$ ($i = 1,\ldots,s$) are s independent states of self-stress, that is an orthonormal basis of the Nullspace of $\mathbf{A}$; $\mathbf{S}$ is the self-stress matrix arranged by $\mathbf{S} = [\mathbf{s}_1\,\mathbf{s}_2\ldots\mathbf{s}_s]$; $\boldsymbol{\alpha}$ is the vector consists of combination coefficients α_i which are free to take any values theoretically and need to be determined further.

2.2. Integral symmetric states of self-stress

In practical situations, tensegrity structures usually have symmetric properties, i.e. invariance conditions by reflection with respect to some planes and/or rotation around some axes, which should be taken into account for the determination of prestress distribution. For instance, it should be noted that the class of prismatic tensegrities designed in previous section have rotational symmetric properties, e.g. satisfy the invariance condition to rotation around z-axis by $2i\pi/v$ ($i = 1,\ldots,v$-1). Accordingly, the members can be divided into four groups totally, i.e., horizontal cables, vertical cables, added cables and struts, because all members in each group are located at symmetrical positions – one member in each group can be transformed to any other member of that group by a proper rotational operation. Therefore, the same prestressing force should be assigned to members in the same group, which can be regarded as constraints on prestress distribution deriving from symmetric property. Yuan and Dong (2003) defined it as integral symmetric state of self-stress.

Denote the space of self-stress states (i.e. the Nullspace of $\mathbf{A}$) by $\mathbf{U}_{ss}$. In this section, it will be proved that integral symmetric states of self-stress also span a vector space which is the subset of $\mathbf{U}_{ss}$. Meanwhile, the computation of the vectorial bases for that subspace is also discussed.

Considering a tensegrity structure with g groups of members, an integral symmetric state $\widehat{\mathbf{n}}$ should has the form as (Yuan and Dong, 2003)

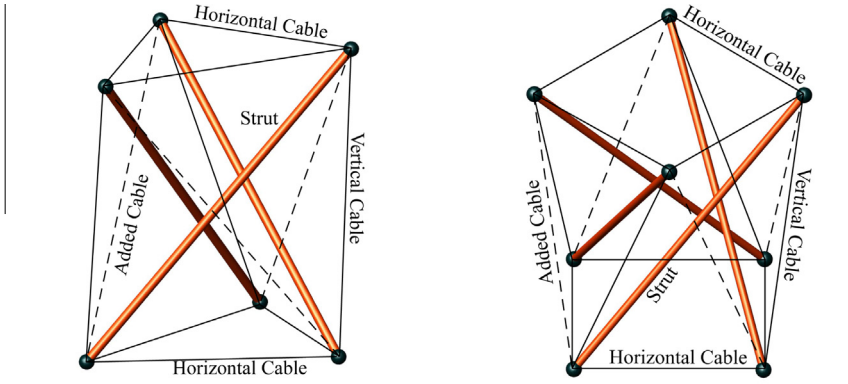

(a) Triangular prismatic tensegrity (b) Quadrangular prismatic tensegrity

Fig. 3. The arrangement of added cables.

Table 1
The number of states of self-stress and independent mechanisms in prismatic tensegrities.[1]

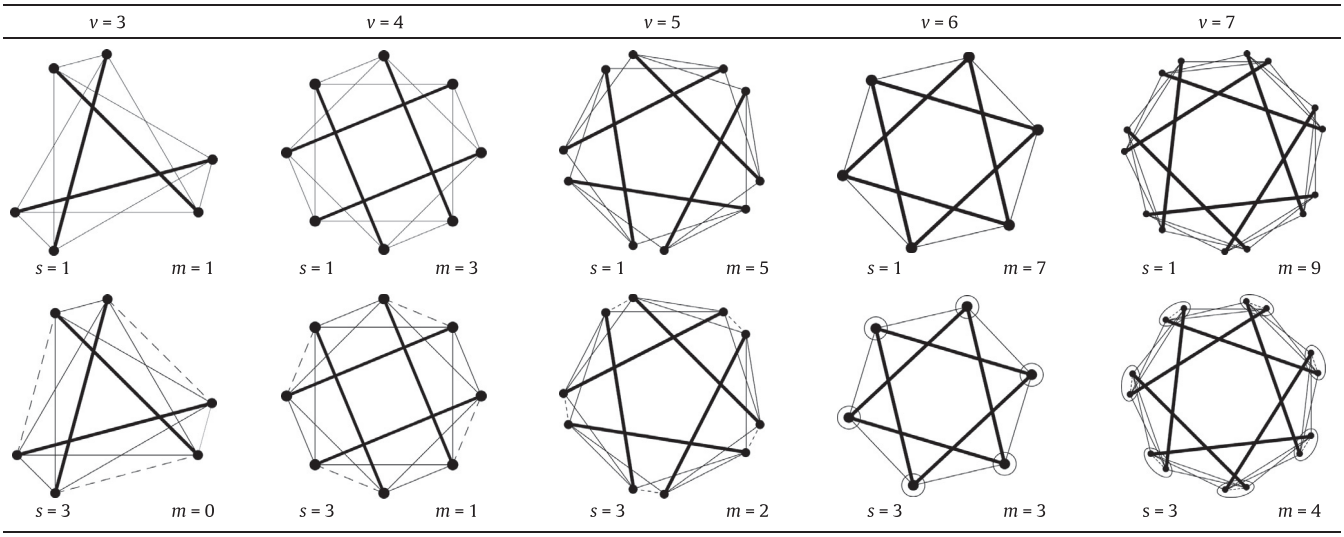

$$\widehat{\mathbf{n}} = \{\beta_1\,\beta_1\,\beta_1 \cdots \beta_i\,\beta_i\,\beta_i \cdots \beta_g\,\beta_g\,\beta_g\}^{\mathrm{T}} = \begin{bmatrix} 1 & 0 & 0 & 0 & 0 \\ \vdots & 1 & 0 & 0 & 0 \\ 0 & \vdots & 1 & 0 & 0 \\ 0 & 0 & \vdots & 1 & \vdots \\ 0 & 0 & 0 & \vdots & 1 \end{bmatrix}_{b\times g} \begin{Bmatrix} \beta_1 \\ \vdots \\ \beta_i \\ \vdots \\ \beta_g \end{Bmatrix}_{g\times 1} \tag{5}$$

where β_i is the tension of members associated with i-th group.

For simplification, Eq. (5) can be rewritten as

$$\widehat{\mathbf{n}} = [\mathbf{e}_1\,\mathbf{e}_2 \cdots \mathbf{e}_g]\,\boldsymbol{\beta} \tag{6}$$

in which $\boldsymbol{\beta} = \{\beta_1 \ldots \beta_i \ldots \beta_g\}^{\mathrm{T}}$ is the tension vector of g groups; and $\mathbf{e}_i$ is the basis vector composed of a unit in i-th group and zero in other groups which has the form:

$$\mathbf{e}_i = [0 \cdots 0\ \underbrace{1 \cdots 1}_{ith\ group}\ 0 \cdots 0]^{\mathrm{T}} \tag{7}$$

Herein it is recommended to normalize the basis vectors $\mathbf{e}_i$ (i = 1,2,...,g) in advance as

$$\bar{\mathbf{e}}_i = \mathbf{e}_i / \sqrt{\mathbf{e}_i^{\mathrm{T}}\mathbf{e}_i} \tag{8}$$

After that, an integral symmetric state $\widehat{\mathbf{n}}$ can also be expressed as

$$\widehat{\mathbf{n}} = [\bar{\mathbf{e}}_1\,\bar{\mathbf{e}}_2 \ldots \bar{\mathbf{e}}_g]\,\boldsymbol{\beta} \tag{9}$$

The major difference of Eq. (9) with respect to Eq. (6) is that the matrix $[\bar{\mathbf{e}}_1\,\bar{\mathbf{e}}_2\,\ldots\,\bar{\mathbf{e}}_g]$ consisting of normalized vectors satisfies the following equation

$$[\bar{\mathbf{e}}_1\,\bar{\mathbf{e}}_2\,\ldots\,\bar{\mathbf{e}}_g]^T\,[\bar{\mathbf{e}}_1\,\bar{\mathbf{e}}_2\,\ldots\,\bar{\mathbf{e}}_g] = \mathbf{I}_{g\times g} \tag{10}$$

which will provide substantial advantage for computation as shown later.

However, we do not have a free choice for $\boldsymbol{\beta}$ as this vector should guarantee $\widehat{\mathbf{n}}$ satisfy Eq. (5) simultaneously. Hence substituting Eq. (9) into Eq. (5) gives

$$\mathbf{A}\,[\bar{\mathbf{e}}_1\,\bar{\mathbf{e}}_2\,\ldots\,\bar{\mathbf{e}}_g]\,\boldsymbol{\beta} = \mathbf{0} \tag{11}$$

which will be used to determine the variable vector $\boldsymbol{\beta}$. The coefficient matrix $\mathbf{A}[\bar{\mathbf{e}}_1\,\bar{\mathbf{e}}_2\,\ldots\,\bar{\mathbf{e}}_g]$ in Eq. (11) is a $(3n \times g)$ matrix of rank r' and can be regarded as a reduced form of $\mathbf{A}$ constrained by the symmetry conditions. Similarly, all solutions to this linear homogeneous system lie in the Nullspace of $\mathbf{A}[\bar{\mathbf{e}}_1\,\bar{\mathbf{e}}_2\,\ldots\,\bar{\mathbf{e}}_g]$ and have a general form as a linear combination

[1] The figures in Table 1 just show the top view of the structures. Added cables are denoted by dot lines. For the cases of $v = 6$ and $v = 7$, since added cables degenerate to dots or be too short to see from top view, they are marked out by circles particularly.

$$\boldsymbol{\beta} = [\boldsymbol{\beta}_1\ \boldsymbol{\beta}_2 \dots\ \boldsymbol{\beta}_h]\ \boldsymbol{\eta} \tag{12}$$

where $h = g - r$' represents the dimension of the Nullspace of $\mathbf{A}[\bar{\mathbf{e}}_1\ \bar{\mathbf{e}}_2\ \dots\ \bar{\mathbf{e}}_g]$; $\boldsymbol{\beta}_i$ (i = 1,...,h) is an orthonormal basis of this subspace, which can be obtained by using singular value decomposition on $\mathbf{A}[\bar{\mathbf{e}}_1\ \bar{\mathbf{e}}_2\ \dots\ \bar{\mathbf{e}}_g]$; $\boldsymbol{\eta}$ is an arbitrary vector of h real coefficients.

When Substitute Eq. (12) into Eq. (9), the general form of integral symmetric states of self-stress $\widehat{\mathbf{n}}$ is given by

$$\widehat{\mathbf{n}} = [\bar{\mathbf{e}}_1\ \bar{\mathbf{e}}_2 \dots\ \bar{\mathbf{e}}_g]\ [\boldsymbol{\beta}_1\ \boldsymbol{\beta}_2 \dots\ \boldsymbol{\beta}_h]\ \boldsymbol{\eta} \tag{13}$$

And Eq. (13) can be further simplified as

$$\widehat{\mathbf{n}} = \left[\widehat{\mathbf{s}}_1\ \widehat{\mathbf{s}}_2 \dots\ \widehat{\mathbf{s}}_h\right]\ \boldsymbol{\eta} \tag{14}$$

where $\widehat{\mathbf{s}}_i = [\bar{\mathbf{e}}_1\ \bar{\mathbf{e}}_2 \dots\ \bar{\mathbf{e}}_g]\ \boldsymbol{\beta}_i$ ($i = 1,2,\dots,h$) are linearly independent vectors since the following equations hold (Eq. (10) is used to get following relationship)

$$\widehat{\mathbf{s}}_i^T \widehat{\mathbf{s}}_j = \boldsymbol{\beta}_i\ [\bar{\mathbf{e}}_1\ \bar{\mathbf{e}}_2 \dots\ \bar{\mathbf{e}}_g]^T\ [\bar{\mathbf{e}}_1\ \bar{\mathbf{e}}_2 \dots\ \bar{\mathbf{e}}_g]\ \boldsymbol{\beta}_j = \boldsymbol{\beta}_i^T\ \boldsymbol{\beta}_j = \begin{cases} 1 & i = j \\ 0 & i \neq j \end{cases} \tag{15}$$

It indicates that all integral symmetric states of self-stress precisely constitute a vector space spanned by $\widehat{\mathbf{s}}_i$ (i = 1,2,...,h). We denote it as $\mathbf{U}_{\text{iss}}$ (Compare to the Nullspace of $\mathbf{A}$ denoted as $\mathbf{U}_{\text{ss}}$, which contains all states of self-stress). Since each $\widehat{\mathbf{n}} \in \mathbf{U}_{\text{iss}}$ certainly belong to $\mathbf{U}_{\text{ss}}$ (i.e. satisfy the condition of $\widehat{\mathbf{n}} \in \mathbf{U}_{ss}$), $\mathbf{U}_{\text{iss}}$ is the subset of $\mathbf{U}_{\text{ss}}$, i. e.

$$\mathbf{U}_{\text{iss}} \subseteq \mathbf{U}_{\text{ss}} \quad \& \quad h(= g - r') \leqslant s(= b - r) \tag{16}$$

which indicates that the total number of variables in initial self-stress design is reduced by taking into account the symmetric properties of the structures.

2.3. Energy method for the determination of integral symmetric prestress

An algorithm to compute the vectorial bases associated with integral symmetric states of self-stress has been described in previous section. Very similar approach also can be found in Yuan and Dong (2003) and Tran and Lee (2010). The common feature of them is that the correct group division of members is required to guarantee the accuracy of results, i.e., the final results are sensitive to grouping. However, because the member groups are directly assigned by designers in terms of geometric symmetry of the structures, this approach may suffer from difficulties or make mistakes when applied to, for example, the structures where the topological relationships of members are complicated and the symmetric properties cannot be observed readily. In this section, a set of self-stress states satisfying the stationary condition of initial strain energy are first obtained by using eigenvalue analysis of a certain matrix. Further discussion shows that an orthonormal basis spanning the space of integral symmetric states of self-stress are included automatically without using any additional constraint deriving from symmetric property, e.g. the classification of members as previous works.

For a tensegrity structure made up of b members, the axial flexibility matrix is defined as $\mathbf{F} = \text{diag}\ (l_1/(E_1A_1),\dots,l_b/(E_bA_b))$, where E_k, A_k, l_k denote Young's modulus, cross-sectional area and length of k-th member respectively. Even if E_k and A_k are unknown, we can also suppose that the product of them is equal to a unit and hence the expression of axial flexibility matrix is simplified as $\mathbf{F} = \text{diag}\ (l_1,\dots,l_b)$. Then the total initial strain energy of the structure, which is the sum of strain energy for each member, can be expressed as

$$\Pi = \sum_{i=1}^{b} \frac{n_i^2 \cdot l_i}{2E_iA_i} = \frac{1}{2}\mathbf{n}^{\mathrm{T}}\mathbf{F}\mathbf{n} \tag{17}$$

Substituting Eq. (4) into Eq. (17) gives

$$\Pi(\boldsymbol{\alpha}) = \frac{1}{2}\boldsymbol{\alpha}^{\mathrm{T}}\mathbf{S}^{\mathrm{T}}\mathbf{F}\mathbf{S}\boldsymbol{\alpha} \tag{18}$$

Since the minimum initial strain energy indicates the least external work produced by tensioning equipment, we consider finding certain $\boldsymbol{\alpha}$ which satisfy the stationary condition of functional Π. However, it can be seen from Eq. (18) that the smaller the Euclidean norm of $\boldsymbol{\alpha}$ is, the smaller the value of Π is. To eliminate this effect, the normalization condition $\boldsymbol{\alpha}^{\mathrm{T}}\boldsymbol{\alpha} = 1$ is introduced into Eq. (18) by using Lagrange multiplier method and the following functional is obtained

$$\Pi(\boldsymbol{\alpha}, \lambda) = \frac{1}{2}\boldsymbol{\alpha}^{\mathrm{T}}\mathbf{S}^{\mathrm{T}}\mathbf{F}\mathbf{S}\boldsymbol{\alpha} - \frac{1}{2}\lambda(\boldsymbol{\alpha}^{\mathrm{T}}\boldsymbol{\alpha} - 1) \tag{19}$$

Herein we use $\lambda/2$ to represent the Lagrange multiplier, which has no influence on subsequent analysis but make λ just correspond to the eigenvalue of a certain matrix as shown later. The stationary condition of Eq. (19) with respect to the undetermined vector $\boldsymbol{\alpha}$ is given as

$$\frac{\partial \Pi(\boldsymbol{\alpha}, \lambda)}{\partial \boldsymbol{\alpha}} = 0 \tag{20}$$

which yields

$$\mathbf{S}^{\mathrm{T}}\mathbf{F}\mathbf{S}\boldsymbol{\alpha} = \lambda\,\boldsymbol{\alpha} \tag{21}$$

Eq. (21) indicates that the eigenvectors of the matrix $\mathbf{S}^{\mathrm{T}}\mathbf{F}\mathbf{S}$ are the solution of Eq. (20). Noting that $\mathbf{S}^{\mathrm{T}}\mathbf{F}\mathbf{S}$ is a real symmetric matrix of s order, it has s orthonormal eigenvectors which can be obtained through eigenvalue decomposition as

$$\mathbf{S}^{\mathrm{T}}\mathbf{F}\mathbf{S} = [\boldsymbol{\alpha}_1\ \cdots\ \boldsymbol{\alpha}_s]\ \text{diag}(\lambda_1\ \cdots\ \lambda_s)\ [\boldsymbol{\alpha}_1\ \cdots\ \boldsymbol{\alpha}_s]^{\mathrm{T}} \tag{22}$$

Moreover the half of each eigenvalue $\lambda_i/2$ (i = 1,...,s) corresponds to initial strain energy associated with $\boldsymbol{\alpha}_i$ since the following equation holds by replacing λ, $\boldsymbol{\alpha}$ with λ_i, $\boldsymbol{\alpha}_i$ in Eq. (21) and left multiplying $\boldsymbol{\alpha}_i^{\mathrm{T}}/2$ in both sides

$$\Pi(\boldsymbol{\alpha}_i) = \frac{1}{2}\boldsymbol{\alpha}_i^{\mathrm{T}}\mathbf{S}^{\mathrm{T}}\mathbf{F}\mathbf{S}\boldsymbol{\alpha}_i = \lambda_i/2 \tag{23}$$

So far, we have got s states of self-stress satisfying the stationary condition of functional Π denoted as $\mathbf{S}\boldsymbol{\alpha}_1$, $\mathbf{S}\boldsymbol{\alpha}_2$,...,$\mathbf{S}\boldsymbol{\alpha}_s$ which are orthogonal with each other. Next we intend to show that among them the independent states of self-stress satisfying integral symmetry are always included automatically. One may doubt about it since no additional conditions associated with integral symmetry are considered directly to obtain the results above. However, the relation between the symmetric properties of structures and eigenvalue analysis of $\mathbf{S}^{\mathrm{T}}\mathbf{F}\mathbf{S}$, which is not immediately obvious, will be revealed below.

According to the discussion of Section 2.2, any integral symmetric state $\widehat{\mathbf{n}}$ should satisfy Eq. (4) and Eq. (9) simultaneously, i. e.

$$\widehat{\mathbf{n}} = [\bar{\mathbf{e}}_1\ \bar{\mathbf{e}}_2 \dots\ \bar{\mathbf{e}}_g]\ \boldsymbol{\beta} = \mathbf{S}\boldsymbol{\alpha} \tag{24}$$

To guarantee the existence of a solution for vector $\boldsymbol{\beta}$, the vector $\boldsymbol{\alpha}$ containing combination factors should satisfy the following equations based on linear-algebraic theory

$$(\mathbf{I}_{b\times b} - [\bar{\mathbf{e}}_1\ \bar{\mathbf{e}}_2\ \dots\ \bar{\mathbf{e}}_g][\bar{\mathbf{e}}_1\ \bar{\mathbf{e}}_2\ \dots\ \bar{\mathbf{e}}_g]^{+})\mathbf{S}\boldsymbol{\alpha} = \mathbf{0} \tag{25}$$

where $\mathbf{I}_{b\times b}$ is $b \times b$ identity matrix and the superscript " + " represents Moore–Penrose generalized inverse. Since $[\bar{\mathbf{e}}_1\ \bar{\mathbf{e}}_2\ \dots\ \bar{\mathbf{e}}_g]$ is of full column rank, it is straightforward to prove the following relationship by applying Eq. (10)

$$\begin{aligned}[\bar{\mathbf{e}}_1\ \bar{\mathbf{e}}_2\ \dots\ \bar{\mathbf{e}}_g]^{+} &= ([\bar{\mathbf{e}}_1\ \bar{\mathbf{e}}_2\ \dots\ \bar{\mathbf{e}}_g]^T[\bar{\mathbf{e}}_1\ \bar{\mathbf{e}}_2\ \dots\ \bar{\mathbf{e}}_g])^{-1}[\bar{\mathbf{e}}_1\ \bar{\mathbf{e}}_2\ \dots\ \bar{\mathbf{e}}_g]^T \\ &= [\bar{\mathbf{e}}_1\ \bar{\mathbf{e}}_2\ \dots\ \bar{\mathbf{e}}_g]^T\end{aligned} \tag{26}$$

Hence Eq. (25) can be tidied up as

$$[\bar{\mathbf{e}}_1\ \bar{\mathbf{e}}_2 \dots \bar{\mathbf{e}}_g][\bar{\mathbf{e}}_1\ \bar{\mathbf{e}}_2 \dots \bar{\mathbf{e}}_g]^T\mathbf{S}\boldsymbol{\alpha} = \mathbf{S}\boldsymbol{\alpha} \tag{27}$$

And the following equation is obtained by left multiplying $\mathbf{S}^T$ in both sides of Eq. (27)

$$\mathbf{S}^T[\bar{\mathbf{e}}_1\ \bar{\mathbf{e}}_2 \dots \bar{\mathbf{e}}_g][\bar{\mathbf{e}}_1\ \bar{\mathbf{e}}_2 \dots \bar{\mathbf{e}}_g]^T\mathbf{S}\boldsymbol{\alpha} = \boldsymbol{\alpha} \tag{28}$$

Eq. (28) demonstrates that we can employ the eigenvectors of $\mathbf{S}^T[\bar{\mathbf{e}}_1\ \bar{\mathbf{e}}_2 \dots \bar{\mathbf{e}}_g][\bar{\mathbf{e}}_1\ \bar{\mathbf{e}}_2 \dots \bar{\mathbf{e}}_g]^T\mathbf{S}$ (particularly, the eigenvectors should correspond to eigenvalue of 1) as the combination coefficients vector $\boldsymbol{\alpha}$ to obtain the symmetric states of self-stress. But actually the eigenvectors of $\mathbf{S}^T\mathbf{F}\mathbf{S}$ rather than the ones of $\mathbf{S}^T[\bar{\mathbf{e}}_1\ \bar{\mathbf{e}}_2 \dots \bar{\mathbf{e}}_g][\bar{\mathbf{e}}_1\ \bar{\mathbf{e}}_2 \dots \bar{\mathbf{e}}_g]^T\mathbf{S}$ were employed to gain the results before. Recalling this, the distinct parts of these two matrices are extracted and be compared as follows.

It can be easily verified that the matrix $[\bar{\mathbf{e}}_1\ \bar{\mathbf{e}}_2 \dots \bar{\mathbf{e}}_g][\bar{\mathbf{e}}_1\ \bar{\mathbf{e}}_2 \dots \bar{\mathbf{e}}_g]^T$ has the block-diagonal form as

$$[\bar{\mathbf{e}}_1\ \bar{\mathbf{e}}_2 \dots \bar{\mathbf{e}}_g][\bar{\mathbf{e}}_1\ \bar{\mathbf{e}}_2 \dots \bar{\mathbf{e}}_g]^T = \begin{bmatrix} \frac{1}{c_1} \times \mathrm{ones}(c_1) & & & \mathbf{0} \\ & \ddots & & \\ & & \frac{1}{c_i} \times \mathrm{ones}(c_i) & \\ \mathbf{0} & & & \ddots \\ & & & \frac{1}{c_g} \times \mathrm{ones}(c_g) \end{bmatrix} \tag{29}$$

where each submatrix block is associated with a member group and c_i is the total number of members in i-th group. The symbol "ones (c_i)" represents a square matrix of order c_i, in which each entry is a unit, i. e.

$$\mathrm{ones}(c_i) = \underbrace{\begin{bmatrix} 1 & \cdots & 1 \\ \vdots & \dots & \vdots \\ 1 & \cdots & 1 \end{bmatrix}}_{c_i \times c_i} \tag{30}$$

On the other hand, because the members in each group have the same length as well as axial flexibility (denoted by $(l/EA)_i$ for i-th group), the diagonal matrix $\mathbf{F}$ may has the following form

$$\mathbf{F} = \begin{bmatrix} \left(\frac{l}{EA}\right)_1 \times \mathbf{I}_{c_1 \times c_1} & & & \mathbf{0} \\ & \ddots & & \\ & & \left(\frac{l}{EA}\right)_i \times \mathbf{I}_{c_i \times c_i} & \\ \mathbf{0} & & & \ddots \\ & & & \left(\frac{l}{EA}\right)_g \times I_{c_g \times c_g} \end{bmatrix} \tag{31}$$

which can also provide the information of geometric symmetry of the structures, i.e. play the similar role as matrix $[\bar{\mathbf{e}}_1\ \bar{\mathbf{e}}_2 \dots \bar{\mathbf{e}}_g][\bar{\mathbf{e}}_1\ \bar{\mathbf{e}}_2 \dots \bar{\mathbf{e}}_g]^T$. Therefore the independent symmetric states of self-stress are always included in the results obtained through eigenvalue analysis of $\mathbf{S}^T\mathbf{F}\mathbf{S}$.

The key feature of this approach is that we do not consider the effect of symmetry directly so that some symmetry-related operations performed in previous works, e.g. grouping members are avoided. Hence it may have the potential advantage over existing methods when applied to, for example, the structures where the topological relationships of members are complicated and the symmetric properties cannot be observed readily. Meanwhile the obtained symmetric states of self-stress also satisfy the stationary condition of initial strain energy, which is more acceptable for us from practical perspective. Finally, the full procedure of this approach is summarized as follows:

(1) Compute the independent states of self-stress $\mathbf{s}_i$ ($i = 1,\dots,s$) through singular value decomposition of $\mathbf{A}$ and arrange them by columns to obtain the self-stress matrix $\mathbf{S}$;
(2) Assemble the axial flexibility matrix as $\mathbf{F} = \mathrm{diag}\ (l_1/(E_1A_1), \dots, l_b/(E_bA_b))$. If E_k and A_k are unknown, make the simplification of $\mathbf{F} = \mathrm{diag}\ (l_1,\dots,l_b)$;
(3) Perform eigenvalue decomposition for symmetric matrix $\mathbf{S}^T\mathbf{F}\mathbf{S}$ and employ s orthonormal eigenvectors as combination coefficients vector $\boldsymbol{\alpha}$ to get s independent states of self-stress as $\mathbf{S}\boldsymbol{\alpha}_1, \mathbf{S}\boldsymbol{\alpha}_2, \dots, \mathbf{S}\boldsymbol{\alpha}_s$, which satisfy the stationary condition of initial strain energy;
(4) Select the states satisfying integral symmetry from the results obtained in step (3).

2.4. Application

Consider the set of prismatic tensegrity structures defined in Section 2.1 (up to 7 struts). It is assumed herein that the radius of the horizontal circle and the height of the structure satisfy $R = 5$ and $H = 10$ respectively. After step (1) and step (2) listed in previous section, the symmetric matrix $\mathbf{S}^T\mathbf{F}\mathbf{S}$ of s order can be obtained for each case. Obviously, it has three eigenvalues totally since each case contains three independent states of self-stress according to Table 1. When eigenvalue decomposition is carried out for $\mathbf{S}^T\mathbf{F}\mathbf{S}$ as follows

$$\mathbf{S}^T\mathbf{F}\mathbf{S} = [\boldsymbol{\alpha}_1\ \boldsymbol{\alpha}_2\ \boldsymbol{\alpha}_3]\ \mathrm{diag}(\lambda_1\ \lambda_2\ \lambda_3)\ [\boldsymbol{\alpha}_1\ \boldsymbol{\alpha}_2\ \boldsymbol{\alpha}_3]^T \tag{32}$$

three eigenvalues λ_i ($i = 1,2,3$) and corresponding eigenvectors $\boldsymbol{\alpha}_i$ ($i = 1,2,3$) are obtained. By adopting $\boldsymbol{\alpha}_i$ ($i = 1,2,3$) as the combination coefficients vector, we get three orthogonal states of self-stress as $\mathbf{S}\boldsymbol{\alpha}_1$, $\mathbf{S}\boldsymbol{\alpha}_2$, $\mathbf{S}\boldsymbol{\alpha}_3$ respectively. Next we remark that one of them satisfies the integral symmetry naturally, i.e., members at symmetrical positions have the same prestress. The results are shown in Table 2.

In order to verify the accuracy of the proposed method, the approach based on the classification of members (see Section 2.2) is also carried out for the same structures to determine their prestress distribution. Noting that all members can be packed into four groups in terms of geometric symmetry of the structures (see also Section 2.2), we form four normalized basis vector $\bar{\mathbf{e}}_i$ ($i = 1,\dots,4$) (each one corresponds to a certain member group) through Eq. (7) and Eq. (8), and arrange them by columns to assemble the matrix $[\bar{\mathbf{e}}_1\ \dots\ \bar{\mathbf{e}}_4]$. Then it is ascertained that the rank of $\mathbf{A}[\bar{\mathbf{e}}_1\ \dots\ \bar{\mathbf{e}}_4]$ is equal to three, i.e., $r' = 3$. Thus the symmetric state of self-stress $\widehat{\mathbf{n}}$ can be computed by $\widehat{\mathbf{n}} = [\bar{\mathbf{e}}_1\ \dots\ \bar{\mathbf{e}}_4]\ \boldsymbol{\beta}_1\boldsymbol{\eta}$ according to Eq. (13), where $\boldsymbol{\beta}_1$ is the single basis of the Nullspace of $\mathbf{A}\ [\bar{\mathbf{e}}_1\ \dots\ \bar{\mathbf{e}}_4]$ and η degenerate to the factor of prestress level. Indeed, it coincides exactly with the results shown in Table 2.

It can be seen from Table 2 that the prestressing force in added cables is zero for each case. Accordingly, the prestressing forces in other members would coincide with the single state of self-stress of corresponding classic ones. It is clear that the added cables could be put into the assembly in a state of tension by imagining that each of them is a little shorter than the distance between the two joints which it is to connect, and that tension is necessary to provide the small elastic elongation which is required to make the added cables fit. Then the conditions of equilibrium would require other members to change stress also, meanwhile the shape as well as the mechanical properties of the structures are modified. It motivates us to propose a special scheme in next section for the purpose of structural control.

Table 2
Integral symmetric prestress of prismatic tensegrities with added cables.

		$v = 3$	$v = 4$	$v = 5$	$v = 6$	$v = 7$
Eigenvalue (λ)		12.0648	11.7274	11.4890	11.3216	11.2001
Eigenvector ($\boldsymbol{\alpha}$)		$\begin{pmatrix}0.9344\\0.0428\\0.3537\end{pmatrix}$	$\begin{pmatrix}0.0292\\-0.8754\\-0.4826\end{pmatrix}$	$\begin{pmatrix}-0.0563\\-0.9581\\-0.2808\end{pmatrix}$	$\begin{pmatrix}-0.4483\\-0.2420\\-0.8605\end{pmatrix}$	$\begin{pmatrix}0.4017\\0.4577\\0.7932\end{pmatrix}$
Symmetric State of Self-stress ($\mathbf{S\alpha}$)	Horizontal Cables	0.1543	0.1336	0.1195	0.1091	0.1010
	Vertical Cables	0.3188	0.2862	0.2625	0.2440	0.2288
	Added Cables	0	0	0	0	0
	Struts	−0.4291	−0.3639	−0.3202	−0.2887	−0.2647

3. A cable-controlled reconfiguration procedure

3.1. A two stage scheme for reconfiguration

Consider now the following scenario: firstly (i) form the classic prismatic tensegrities with certain prestress level; then (ii) additional cables, the lengths of which are assumed to be adjustable, are used to pull pairs of nodes closer together and modify the geometry and self-stress in the system. Actually such scenario was employed in the construction of a full-scale model with triangular prismatic form, mainly for the improvement of structural stiffness (Kawaguchi and Lu, 2002, Kawaguchi, 2003) and certainly can be extended to other forms of this class, e.g. quadrangular prismatic tensegrity shown in Fig. 4. Furthermore, it should be noted that the modification of cable lengths can be accomplished by motors attached, for example, at the middle of the cables. We consider that these motors work in the following way: the motor pulls a cable and rolls it over a small wheel that its active length is shortened. In such a way, the part of the cable which is rolled over the motor wheel no longer contributes to the cable tension. Hence this control procedure works as if the rest-length of the cable would be shortened.

There are two advantages at least to employ this two-stage scheme for structural control: firstly, (i) it's not so difficult to introduce the prestress into each classic prismatic tensegrity due to its single state of self-stress; secondly, (ii) since the prestressing rigidity of the structure has already been established in the first stage, the structure just evolves from initial equilibrium configuration to a new equilibrium configuration during the second stage, which is defined as reconfiguration in Sultan et al. (2002). By adopting the imposed length change as the control parameters and shortening added cables slowly enough, this reconfiguration procedure can be regarded as a quasi-static process, consisting of a sequence of equilibrium configurations with varying control parameters.

In next section, the governing equation relating nodal displacements and imposed length change of members, as well as the corresponding nonlinear iterative program based on Newton–Raphson method is developed, in order to determine the equilibrium configuration corresponding to each discrete control parameter point, i.e. simulate and follow the process of reconfiguration (Table 3).

3.2. Predictive model

3.2.1. Fundamental assumptions

In this section, the tangent stiffness matrix **K** will be derived for two purposes: 1. establish the relationship between nodal displacements (to first order) and driving force caused by imposed adjustments of member lengths so that provide a means for predicting the structural response during the process of reconfiguration; 2. the smallest eigenvalue of **K** is used subsequently to evaluate the rigidity of the structures since it is associated with the most flexible mode of displacements (Guest, 2011). Before that, the fundamental assumptions are first stated as follows:

(a) Members are connected by pin joints;
(b) Both cables and struts are assumed to have linear elastic stress–strain relationship;
(c) Self-weight of the structure is neglected;
(d) Both local and global buckling are not considered.

3.2.2. Matrix formulation of tangent stiffness

The tangent stiffness formulation appeared in Argyris and Scharpf (1972), and has been used in much work since; an

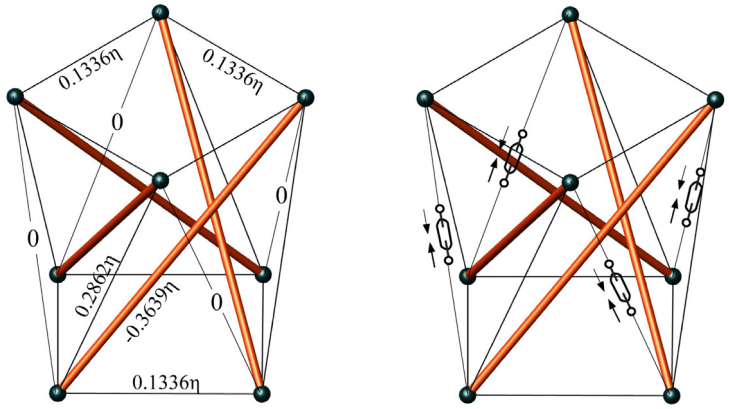

Fig. 4. A two stage scheme for reconfiguration (η is the factor of prestress level).

Table 3
Structural size and material properties.

Member type	Initial length (m)	Material properties, etc.
Horizontal Cables	7.071	$EA_c = 6.283 \times 10^7$N
Vertical Cables	10.707	
Added Cables	10.707	
Struts	13.615	$EA_s = 1.571 \times 10^9$N

equivalent but extended derivation in the setting of large displacement and large strain has been given by Murakami (2001), using the powerful tools of continuum mechanics. Most recently, similar formulation was derived from the Hessian of the potential elastic energy by Sultan (2013).

In this section, the tangent stiffness matrix **K** is found by differentiating equilibrium expressions at nodes of the structure with respect to nodal positions. This derivation approach is certainly not new, which has already been described in Guest (2006). However, a novel feature in this paper is to use matrix form directly for an entire structure during the derivation, rather than Guest (2006) where the tangent stiffness was initially found for a single bar and then be assembled together for the whole structure. Another feature is that we also formulate the driving force for the procedure of reconfiguration combining with the derivation of **K**, which can consider the effects of imposed length change readily.

It is assumed herein that a tensegrity structure consists of n nodes and b members, unrestrained in three dimensions. The equilibrium equations at nodes of the structure can be written in the form

$$\mathbf{An} = \mathbf{f} \tag{33}$$

where **f** is nodal loads vector made up of the x-, y-, and z-components of the external forces applied at each node. Defining member length vector, force density vector and member length matrix as $l = \{l_k\} \in \Re^b$, $t = \{n_k/l_k\} \in \Re^b$ and $L = diag(l) \in \Re^{b\times b}$ respectively, the vector **n** containing the tension of members can be expressed by

$$\mathbf{n} = \mathbf{Lt} \tag{34}$$

Substituting Eq. (34) into Eq. (33) gives

$$(\mathbf{AL})\mathbf{t} = \mathbf{f} \tag{35}$$

For the left-hand side of Eq. (35), Vassart and Motro (1999) separated the nodal coordinates from **AL** and gave the equivalent form using Kronecher product notation "$\otimes$ " as

$$(\mathbf{AL}) \cdot \mathbf{t} = (\mathbf{I} \otimes \mathbf{\Omega})\mathbf{x} \tag{36}$$

where **I** is three-order identity matrix for three-dimensional structures, **x** is the vector contains the x-, y-, and z-components of the coordinates for each node and the symmetric matrix Ω can be written directly from the force densities (Connelly and Terrell, 1995; Vassart and Motro, 1999). The (i, j)-component Ω (i, j) of Ω is given by

$$\Omega_{ij} = \begin{cases} \sum_k t_{ik} & i = j, \quad node\ i\ and\ node\ k\ connect\ by\ a\ bar \\ -t_{ij} & i \neq j, \quad node\ i\ and\ node\ j\ connect\ by\ a\ bar \\ 0 & others \end{cases} \tag{37}$$

For prestressed structures, it is clear that the tension of members as well as the nodal coordinates may change to equilibrate any load increment $\delta\mathbf{f}$. Hence the incremental form of Eq. (35) is given by (similar formulation can be found in Tanaka and Hangai, 1986)

$$\delta(\mathbf{AL}) \cdot \mathbf{t} + \mathbf{AL} \cdot \delta\mathbf{t} = \delta\mathbf{f} \tag{38}$$

Noting that the mathematical expression of each entry in matrix **AL** only includes components of nodal coordinates or be zero alternatively, δ(**AL**) can be obtained by replacing coordinate components with the corresponding incremental ones in **AL**. Combining with Eq. (36), it is clear that the following equations hold

$$\delta(\mathbf{AL}) \cdot \mathbf{t} = (\mathbf{I} \otimes \mathbf{\Omega}) \cdot \delta\mathbf{x} \tag{39}$$

where $\delta\mathbf{x}$ is the vector of incremental coordinates, describing infinitesimal movements of nodes. Obviously, the matrix $\mathbf{I} \otimes \mathbf{\Omega}$ is equivalent to the so-called geometric stiffness matrix $\mathbf{K}_G$ in conventional finite element formulation since it corresponds to the stiffness due to the reorientation of stressed members. For simplicity, Eq. (39) is rewritten as

$$\delta(\mathbf{AL}) \cdot \mathbf{t} = \mathbf{K}_G \cdot \delta\mathbf{x} \tag{40}$$

Next let us expand the second term in the left side of Eq. (38) further

$$\mathbf{AL} \cdot \delta\mathbf{t} = \mathbf{AL} \cdot \delta(\mathbf{L}^{-1}\mathbf{n}) = \mathbf{AL} \cdot \delta(\mathbf{L}^{-1}) \cdot \mathbf{n} + \mathbf{A} \cdot \delta\mathbf{n} \tag{41}$$

in which the relationship $\mathbf{t} = \mathbf{L}^{-1}\mathbf{n}$ is used. Considering that the differential of $\mathbf{L}^{-1}$ yields

$$\delta(\mathbf{L}^{-1}) = -\mathbf{L}^{-1} \cdot \delta\mathbf{L} \cdot \mathbf{L}^{-1} \tag{42}$$

the following equation holds

$$\mathbf{AL} \cdot \delta(\mathbf{L}^{-1}) \cdot \mathbf{n} = -\mathbf{A} \cdot \delta\mathbf{L} \cdot \mathbf{t} \tag{43}$$

Defining the force density matrix as $\mathbf{T} = \text{diag}(\mathbf{t}) \in \Re^{b\times b}$, we also have the relationship

$$\delta\mathbf{L} \cdot \mathbf{t} = \mathbf{T} \cdot \delta\mathbf{l} \tag{44}$$

where $\delta\mathbf{l}$ is the elongation vector, containing infinitesimal extension of each member. Substitution of Eq. (44) into Eq. (43) yields

$$\mathbf{AL} \cdot \delta(\mathbf{L}^{-1}) \cdot \mathbf{n} = -\mathbf{A} \cdot \mathbf{T} \cdot \delta\mathbf{l} \tag{45}$$

Noting that the kinematic compatibility equations relating $\delta\mathbf{x}$ and $\delta\mathbf{l}$ hold as (Pellegrino and Calladine, 1986)

$$\mathbf{A}^{\mathrm{T}}\delta\mathbf{x} = \delta\mathbf{l} \tag{46}$$

where the contragradient relationship between equilibrium matrix and compatibility matrix is used, Eq. (45) can be rewritten as

$$\mathbf{AL} \cdot \delta(\mathbf{L}^{-1}) \cdot \mathbf{n} = -(\mathbf{ATA}^{\mathrm{T}}) \cdot \delta\mathbf{x} \tag{47}$$

On the other hand, considering that the elongation δl for each member consists of two parts, (i) an inelastic part due to the imposed length change e, and (ii) a linear-elastic part caused by the change of axial force δn, $\delta\mathbf{l}$ and $\delta\mathbf{n}$ are related by

$$\delta\mathbf{l} = \mathbf{e} + \mathbf{F} \cdot \delta\mathbf{n} \tag{48}$$

where the vector **e** contains the imposed elongation e of each member. Hence Eq. (46) can be written in the form

$$\mathbf{A}^{\mathrm{T}}\delta\mathbf{x} = \mathbf{e} + \mathbf{F} \cdot \delta\mathbf{n} \tag{49}$$

which can be tidied up as

$$\delta\mathbf{n} = \mathbf{F}^{-1}\left(\mathbf{A}^{\mathrm{T}}\delta\mathbf{x} - \mathbf{e}\right) \tag{50}$$

Substituting Eqs. (47) and (50) into Eq. (41) yields

$$\mathbf{AL} \cdot \delta\mathbf{t} = (-\mathbf{ATA}^{\mathrm{T}}) \cdot \delta\mathbf{x} + (\mathbf{AF}^{-1}\mathbf{A})^{\mathrm{T}} \cdot \delta\mathbf{x} - \mathbf{AFe} \tag{51}$$

To simplify the notations further, we denote the coefficient matrices -$\mathbf{ATA}^{\mathrm{T}}$ and $\mathbf{AF}^{-1}\mathbf{A}^{\mathrm{T}}$ by $\mathbf{K}_{\mathrm{T}}$ and $\mathbf{K}_{\mathrm{E}}$ respectively, giving

$$\mathbf{AL} \cdot \delta\mathbf{t} = \mathbf{K}_T \cdot \delta\mathbf{x} + \mathbf{K}_E \cdot \delta\mathbf{x} - \mathbf{AF}^{-1}\mathbf{e} \tag{52}$$

where $\mathbf{K}_{\mathrm{E}}$ corresponds to the material stiffness matrix in conventional finite element formulation and $\mathbf{K}_{\mathrm{T}}$ usually can be neglected compared with $\mathbf{K}_{\mathrm{E}}$ since the axial force is generally far less than axial stiffness for each member. Then substitute Eqs. (52) and (40) into Eq. (38) and tidy up as follows

$$(\mathbf{K}_E + \mathbf{K}_G + \mathbf{K}_T) \cdot \delta\mathbf{x} = \delta\mathbf{f} + \mathbf{AF}^{-1}\mathbf{e} \tag{53}$$

When the tangent stiffness matrix $\mathbf{K}$ is given by

$$\mathbf{K} = \mathbf{K}_E + \mathbf{K}_G + \mathbf{K}_T \tag{54}$$

Eq. (53) can be written in simpler form as

$$\mathbf{K} \cdot \delta\mathbf{x} = \delta\mathbf{f} + \mathbf{A}\mathbf{F}^{-1}\mathbf{e} \tag{55}$$

3.2.3. Nonlinear iterative program

It can be observed from Eq. (55) that the nodal displacements are not only caused by an additional load $\delta\mathbf{f}$ but also by the imposed elongation $\mathbf{e}$. Considering that there only exists $\mathbf{e}$ during the reconfiguration procedure described in Section 3.1, $\delta\mathbf{f}$ could be zero and Eq. (55) becomes

$$\mathbf{K} \cdot \delta\mathbf{x} = \mathbf{A}\mathbf{F}^{-1}\mathbf{e} \tag{56}$$

the right-hand side of which is defined as driving force for the procedure of reconfiguration caused by $\mathbf{e}$. Herein we denote it by $\delta\mathbf{f}'$ since it can be treated identically as an additional load $\delta\mathbf{f}$ applied at nodes.

However, noting that the structures considered in this paper are free-standing, i.e., six rigid-body motions are not constrained, the tangent stiffness matrix $\mathbf{K}$ is singular. One of the simplest ideas to overcome this problem is making use of Moore–Penrose generalized inverse to compute the nodal displacements $\delta\mathbf{x}$ as

$$\delta\mathbf{x} = \mathbf{K}^{+} \cdot \mathbf{A}\mathbf{F}^{-1}\mathbf{e} \tag{57}$$

After that, the deformed configuration can be obtained by updating nodal coordinates as follows

$$\mathbf{x}^2 = \mathbf{x}^1 + \delta\mathbf{x} \tag{58}$$

where the nodal coordinate vectors $\mathbf{x}^1$ and $\mathbf{x}^2$ are associated with initial configuration and deformed configuration respectively. Then the member length vector $\mathbf{l}$ and equilibrium matrix $\mathbf{A}$ are also corrected based on the new location $\mathbf{x}^2$.

In addition, recalling that the imposed length adjustment is accomplished as if the rest-length of the cable would be changed (see Section 3.1), the current member tension vector $\mathbf{n}$ can be computed as

$$\mathbf{n} = \mathbf{F}^{-1}(\mathbf{1} - \mathbf{1}^0 - \mathbf{e}) \tag{59}$$

where $\mathbf{l}^0$ is the vector containing rest-length l^0 of each member before the imposed contraction is acted upon. l^0 is approximately equal to the initial length when the prestressing level is low. For the new location, the equilibrium equations (33) are usually not satisfied precisely since the derivation of $\mathbf{K}$ is based upon linear-elasticity hypothesis. Considering zero external load applied to the joints, i.e., $\mathbf{f} = \mathbf{0}$, the out-of-balance forces are given as

$$\delta\mathbf{f}' = \mathbf{f} - \mathbf{A}\mathbf{n} = -\mathbf{A}\mathbf{n} \tag{60}$$

Then a nonlinear program based on Newton–Raphson method which uses the Moore–Penrose generalized inverse of $\mathbf{K}$ within each corrective iteration is presented to eliminate out-of-balance forces $\delta\mathbf{f}'$. The location is corrected iteratively, unless the 2-norm of $\delta\mathbf{f}'$ is less than the allowable error ξ. Finally the deformed configuration and member tensions are obtained. The algorithm is summarized by the flowchart in Fig. 5.

3.3. Example

Consider now the reconfiguration procedure proposed in Section 3.1 for quadrangular prismatic tensegrity with additional cables. The upper part of Fig. 6 gives the initial equilibrium configuration in which additional cables are not yet in tension (Actually it shows the same structure drawn in Fig. 4, but with a coordinate system and node numbering scheme). Note that part of geometric

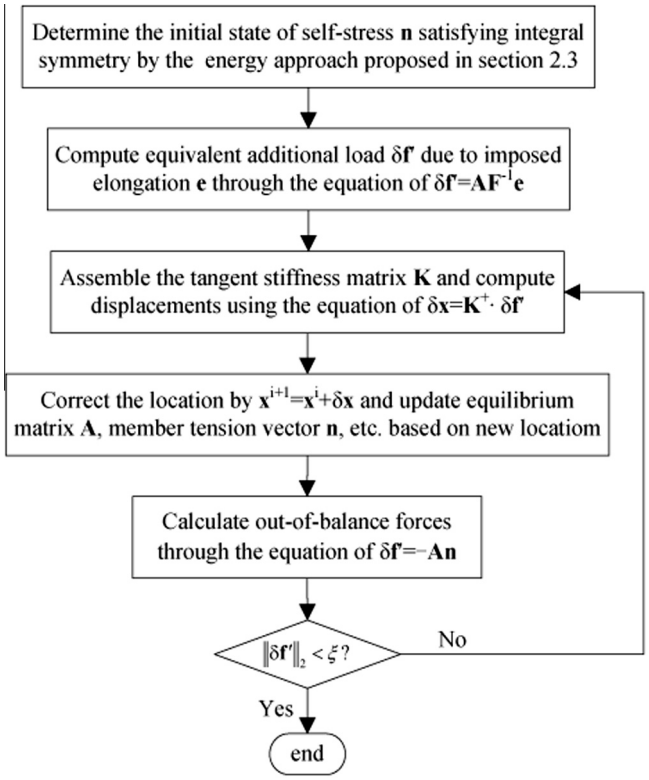

Fig. 5. Flowchart of the nonlinear iterative program.

information of this configuration was given in previous section as $\theta = 45°$, $R = 5$ and $H = 10$. The section size and material properties, which are also necessary for analysis, are complemented as follows: the cross-sectional shape of each member is assumed to be a circle, whose radius is 0.01 m for cables and 0.05 m for struts; Young's modulus of the material is 200e9 Pa. Thus the products of Young's modulus E and cross-sectional area A_c (or A_s) are equal to 6.283×10^7 N for cables and 1.571×10^9 N for struts respectively.

When the normalized symmetric state of self-stress shown in Table 2 for the case of $v = 4$ is denoted by $\hat{s}$, the initial prestress distribution $\hat{\mathbf{n}}$ can be given as (see Eq. (14))

$$\hat{\mathbf{n}} = \eta \cdot \hat{\mathbf{s}} \tag{61}$$

where the prestress level coefficient η is assumed to be determined as

$$\eta = E \cdot A_c/3000 \tag{62}$$

In addition, the following assumptions have been stated before the investigation:

(a) The aim of this numerical analysis is not conventional modeling of structures, but answering questions such as how the structural configuration will vary under imposed lengths change of added cables. Therefore the yield as well as strain limit of structural material are not considered;
(b) Generally we want to change the initial configuration to another symmetrical configuration, which is defined as symmetrical reconfiguration in Sultan et al. (2002). Particularly, the serviceability criteria of maintaining a zero slope for both upper and lower cable planes is hopefully to be guaranteed from a practical perspective (for example, we can imagine a potential application in which the upper level attaches the covering material and the lower level is located on the

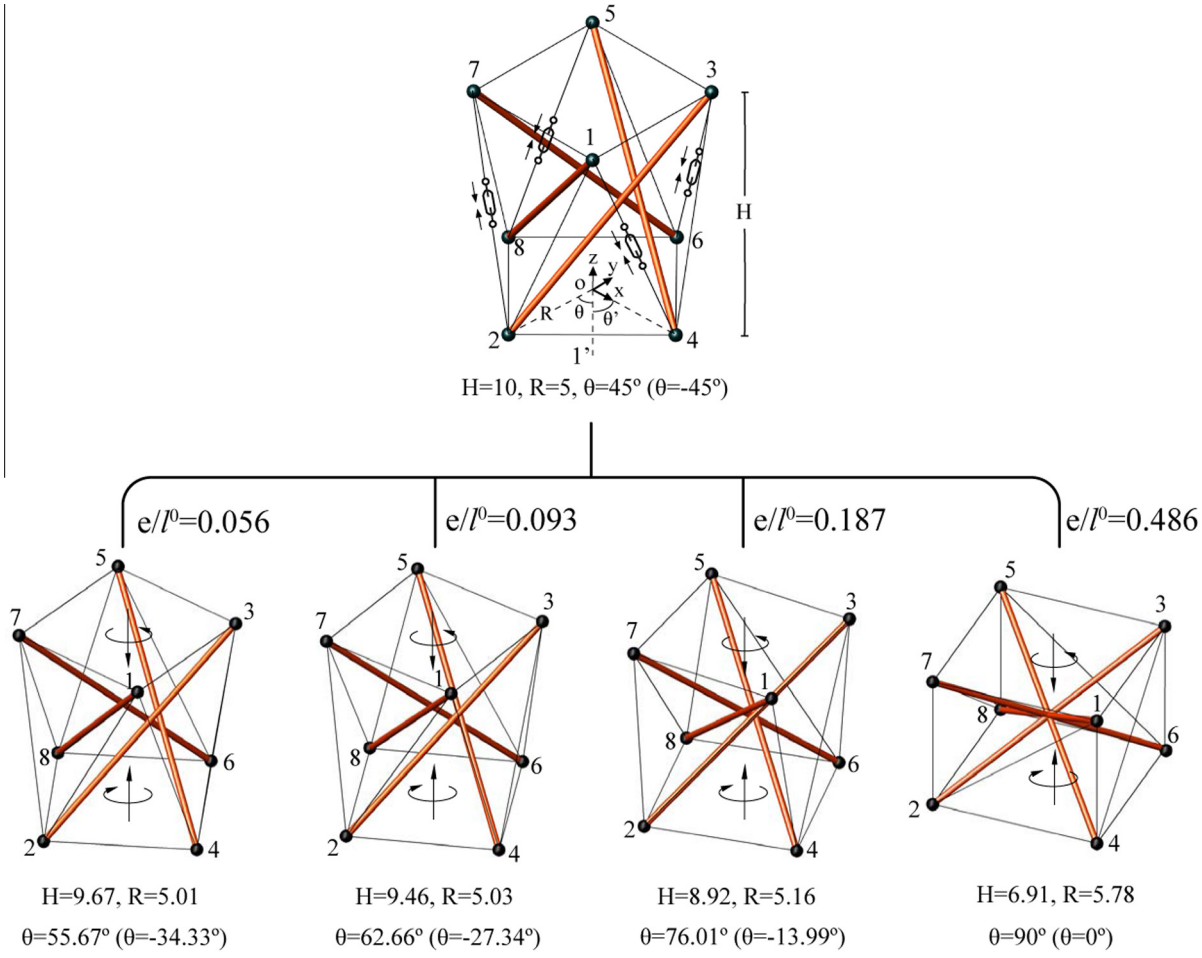

Fig. 6. Deformed configurations for different value of imposed length decrement (Dot 1' is the projection in bottom cable plane from Node 1).

base directly). In order to meet such criteria, the length adjustments for every added cable are assumed to be equal and also be acted upon simultaneously throughout the reconfiguration procedure.

To guarantee the approximation with quasi-static process, consider that the imposed contraction e for each added cable is performed slowly. Thus the reconfiguration process can be regarded as consisting of a sequence of equilibrium configurations with varying e. Then the nonlinear iterative algorithm proposed in previous section is employed to determine these configurations, i.e. to simulate and follow the process of reconfiguration.

As representatives of the results, the lower part of Fig. 6 shows four equilibrium configurations corresponding to different value of e (the single control parameter e is non-dimensionalised by e/l^0 here, where l^0 represents initial length of added cable). The analysis is terminated at the point of $e/l^0 = 0.486$, since the tension in vertical cables just vanish (it will be illustrated later).

By checking the structural geometries, it can be verified that the successive symmetrical configurations the structure passes through during the procedure maintain the initial rotational symmetric property described as the invariance condition to rotation around z-axis by $2i\pi/v$ ($i = 1, \ldots, v\text{-}1$). It means that the symmetrically located members (e.g. all horizontal cables or all struts) in initial configuration are always at symmetrical positions throughout the process and the polygons formed by horizontal cables are kept to be regular polygons (herein they are squares). Thus these configurations can be described exactly by three parameters: the radius of circumcircle – R, the height of the structure – H and the relative rotation angle between two polygons – $\theta = \angle 2o1'$ or the equivalent one $\theta' = \angle 4o1'$ which are always connected by the following equation (see Fig. 6)

$$\theta' = \theta - \frac{360^\circ}{v} \text{ (herein } v = 4) \tag{63}$$

The evolution of H has been provided in Fig. 7, indicating that the height of the structure is decreasing gradually with increasing magnitude of e (the top cable plane translates downwards while

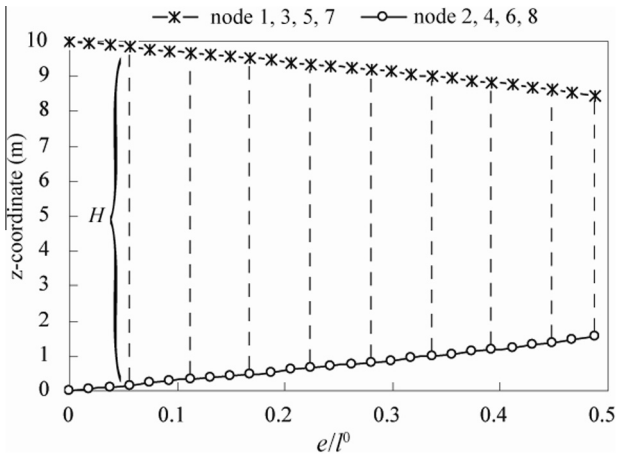

Fig. 7. The development of z-component of nodal coordinates with imposed length decrement.

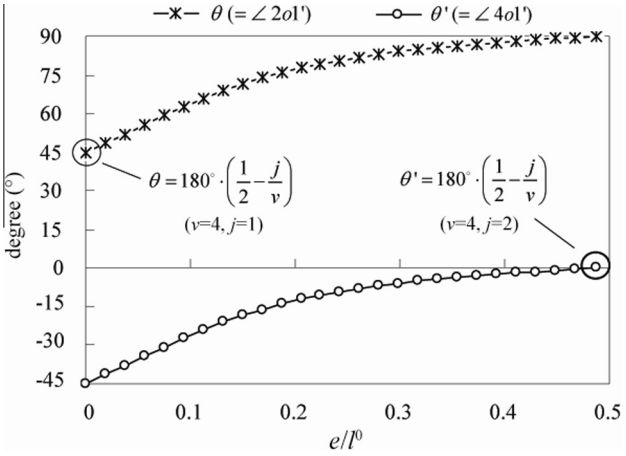

Fig. 8. The development of relative rotation angle with imposed length decrement.

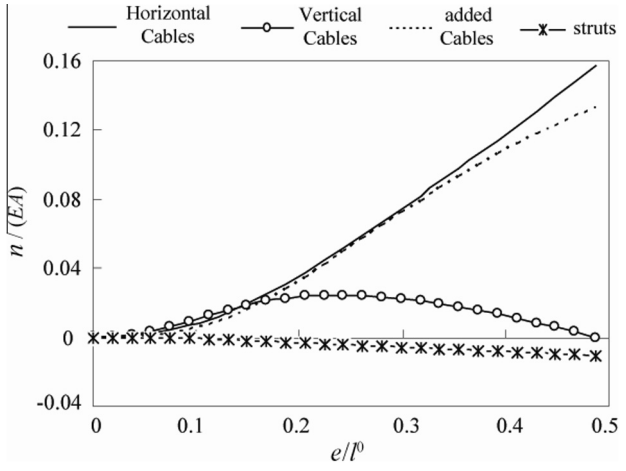

Fig. 9. The development of axial forces with imposed length decrement.

the bottom one translates upwards). Meanwhile, the corresponding $\theta(e/l^0)$ as well as $\theta'(e/l^0)$ is plotted in Fig. 8, showing that the twist angle between two polygons is increasing from $\theta = 45°$ to $\theta = 90°$ during the complete procedure (the top polygon rotates anticlockwise around z-axis while the bottom one rotates clockwise). It is noteworthy that the equilibrium configuration at the final point of $e/l^0 = 0.486$, characterized by $R = 5.78$, $H = 6.91$, $\theta = 90°$ ($\theta' = 0°$), coincides with the equilibrium configuration given by Eq. (1) for the case of $j = 2$. The evidence to verify this is twofold: (1) the tension in vertical cables just vanish implying that they can be eliminated from assembly; (2) θ' satisfy the Eq. (1) in the case of $v = 4$ and $j = 2$.

The development of axial forces with imposed length decrement is provided in Fig. 9 to ascertain that all cables are in tension and all struts are in compression throughout the reconfiguration process. The axial force n is non-dimensionalised by $n/(EA_c)$ for cables and $n/(EA_s)$ for struts, which can be regarded as nominal strain of members. Fig. 9 shows that the tensions in both of the horizontal cables and added cables increase throughout the process, while the tensions in vertical cables increase firstly, but then decrease after e/l^0 exceeds approximately 0.243, and finally vanish at the point of $e/l^0 = 0.486$. When we continue to increase the magnitude of e, the conditions of equilibrium would require vertical cables to carry compression, which is not physically feasible. That's why the analysis is terminated at the point of $e/l^0 = 0.486$ as stated before.

Actually, when the same symmetrical reconfiguration procedure is acted upon on prismatic tensegrities in the cases of $v = 5$, 6, 7, similar results are obtained by using the predictive model proposed before. The key features for this class of structures undergoing such procedures can be summarized as follows. By shortening added cables gradually, the structure evolves from the initial point, where the axial force in added cables is zero, to the final point where the tensions in vertical cables just vanish. Meanwhile, the twist angle between two polygons increases from $\theta = 180°(1/2–1/v)$ to $\theta = 90°$. At the final point characterized by $\theta = 90°$, the following equation holds according to Eq. (63)

$$\theta' = \theta - \frac{360^\circ}{v} = 90^\circ - \frac{360^\circ}{v} = 180^\circ \cdot \left(\frac{1}{2} - \frac{2}{v}\right) \tag{64}$$

It demonstrates that the initial equilibrium configuration corresponding to j = 1 in Eq. (1) is transformed into the final equilibrium configuration corresponding to j = 2 in Eq. (1) (see Fig. 10) through the process of this symmetrical reconfiguration.

Another interesting situation in which this class of symmetrical reconfigurations are very useful is when the structure is required to improve its stiffness with the constraint of maintaining zero slope for both of upper and bottom levels from a practical perspective (for example, we can imagine an application in which the upper level may attach the covering material and the lower level may be located on the base directly). Consider that the smallest eigenvalue of the tangent stiffness matrix is associated with the most flexible mode of displacements (Guest, 2011) and reflects the global stiffness of the structure. A complete overview of the stiffness

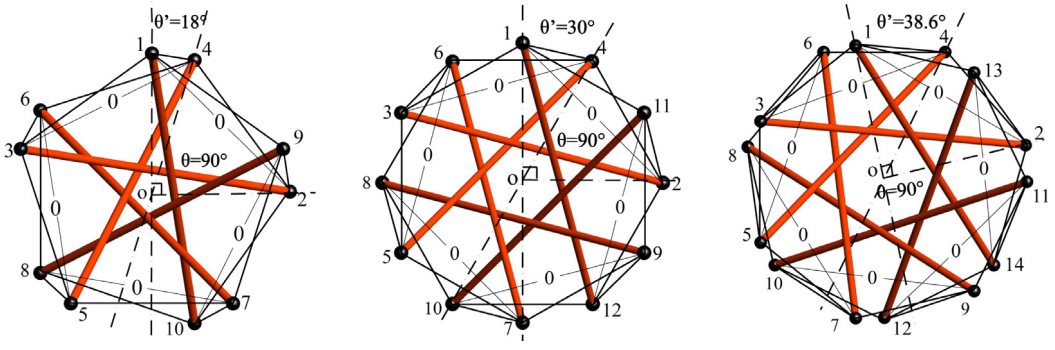

(a) v=5, j=2 (b) v=6, j=2 (c) v=7, j=2

Fig. 10. Top view of the equilibrium configurations obtained by shortening the added cables gradually until the tensions in vertical cables vanish.

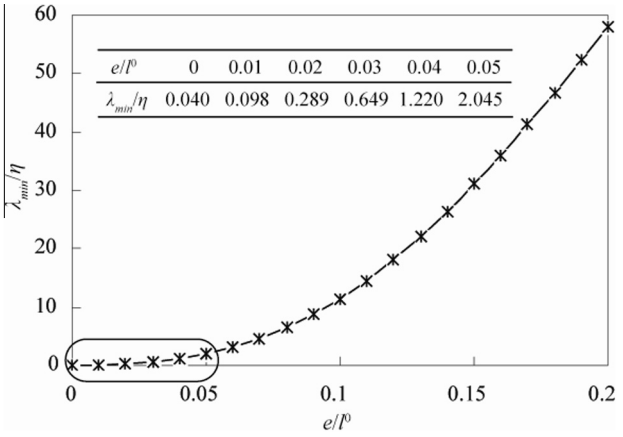

Fig. 11. The plots of the smallest eigenvalues of the tangent stiffness matrix for varying values of e/l^0.

Fig. 12. A full-scale model serving for the skeleton of a membrane structure in Chiba Japan.

change is provided by the plots of the smallest eigenvalues of **K** for $0 < e/l^0 < 0.2$ given in Fig. 11 (6 zero eigenvalues corresponding to rigid body modes are certainly eliminated). To non-dimensionalise the results also, the smallest eigenvalues λ_{min} are plotted relative to the initial prestress level factor η (=$EA_c/3000$).

Fig. 11 shows that the structure becomes stiffer and stiffer gradually. Even the decrement e is only 2% of the initial length l^0, the dimensionless parameter λ_{min}/η changes from 0.040 to 0.289 which is approximately 7 times as large. In this way, they have the potential to become part of an exhibition rather than merely provide shelter for one. Indeed a full-scale laboratory prototype has been built, serving as the skeleton of a real membrane structure (see Fig. 12). During the stiffness modification procedure, 22-ton prestress was introduced manually without any mechanical power, making it meet the serviceability criteria well (Kawaguchi and Lu, 2002, Kawaguchi, 2003).

4. Conclusions

A simple energy method making use of eigenvalue analysis is proposed to determine the symmetric prestress distribution for certain tensegrity structures with multiple states of self-stress. Essentially, it is to achieve a special orthonormal basis spanning the space of integral symmetric states of self-stress, which satisfy the stationary condition of initial strain energy simultaneously. Since the effect of symmetry is not considered directly in this method, certain symmetry-related operations performed in previous works, e.g. grouping members are avoided. Thus it is more convenient to treat the structures with large number of members and complicated topology. A class of prismatic tensegrities with additional cables, which are the variations on the classic ones, are first introduced to show the validity and accuracy of the presented method. Then a cable-controlled reconfiguration procedure is put forward for these structures, in which only additional cables are assumed to be adjustable and provide the driving force to change the shape as well as mechanical properties of the structures. By adopting the length adjustments as the control parameters, this reconfiguration procedure is regarded as a quasi-static process, consisting of a sequence of equilibrium configurations with varying control parameters. In order to determine these configurations (i.e. simulate and follow this reconfiguration process), a governing equation relating nodal displacements and imposed length change of members, as well as the corresponding nonlinear iterative program based on Newton–Raphson method is developed. The Moore–Penrose generalized inverse of tangent stiffness matrix is used within each corrective iteration to treat the situation that the structure is free-standing. As numerical examples, a particular class of reconfigurations coined symmetrical reconfigurations are investigated carefully. It has been shown that the transformation between two self-equilibrium configurations corresponding to $j = 1$ and $j = 2$ respectively in Eq. (1) is performed through these symmetrical reconfigurations. Another potential application of them is to improve the structural stiffness under the condition of maintaining zero slopes for horizontal cable planes of the structure. In this way, the tensegrities investigated in this paper may have the feasibility to become part of an exhibition rather than merely provide shelter for one.

Acknowledgement

The main part of this study was carried out when the first author was visiting the Institute of Industrial Science at the University of Tokyo, supported by State Scholarship Fund from China Scholarship Council (Grant No. 2010609072). The remainder work completed at Southeast University was supported by National Natural Science Foundation of China (Grant No. 51278116). The first author is grateful for financial support from both.

References

Argyris, J.H., Scharpf, D.W., 1972. Large deflection analysis of prestressed networks 98, 633–654.
Calladine, C.R., 1978. Buckminster Fuller's "Tensegrity" structures and Clark Maxwell's rules for the construction of stiff frames. Int. J. Solids Struct. 14, 161–172.
Chen, Y., Feng, J., 2012. Initial prestress distribution and natural vibration analysis of tensegrity structures based on group theory. Int. J. Struct. Stab. Dyn. 12, 213–231.
Connelly, R., Terrell, M., 1995. Globally rigid symmetric tensegrities. J. Struct. Topol. 21, 59–78.
Connelly, R., Back, A., 1998. Mathematics and tensegrity. Amer. Sci. 86, 142–151.
Djouadi, S., Motro, R., Pons, J.C., Crosnier, B., 1998. Active control of tensegrity systems. J. Aerosp. Eng. 11, 37–44.
Fest, E., Shea, K., Domer, B., Smith, I.F.C., 2003. Adjustable tensegrity structures. J. Struct. Eng. 129, 515–526.
Fest, E., Shea, K., Smith, I.F.C., 2004. Active tensegrity structure. J. Struct. Eng. 130, 1454–1465.
Fuller, R. B., 1962. Tensile-integrity structures, United States Patent 3,063,521, November 13.
Guest, S.D., 2011. The stiffness of tensegrity structures. IMA J. Appl. Math. 76, 57–66.
Guest, S., 2006. The stiffness of prestressed frameworks: a unifying approach. Int. J. Solids Struct. 43, 842–854.
Juan, S.H., Mirats Tur, J.M., 2008. Tensegrity frameworks: Static analysis review. Mech. Mach. Theory 43, 859–881.

Kangwai, R.D., Guest, S.D., 2000. Symmetry-adapted equilibrium matrices. Int. J. Solids Struct. 37, 1525–1548.
Kawaguchi, K., Lu Z. Y., 2002. Construction of three-strut tension systems. Proceedings of the Fifth International Conference on Space Structures, Parke G & Disney P (ed.) 1, 1–10.
Kawaguchi, K., 2003. Prestress states of tension-truss and tensegrity. Proceedings of the IASS-APCS, Taipei.
Lee, S., Woo, B., Lee, J., 2014. Self-stress design of tensegrity grid structures using genetic algorithm. Int. J. Mech. Sci. 79, 38–46.
Murakami, H., 2001. Static and dynamic analyses of tensegrity structures. Part II. Quasi-static analysis. Int. J. Solids Struct. 38, 3615–3629.
Pellegrino, S., 1993. Structural computations with the singular value decomposition of the equilibrium matrix. Int. J. Solids Struct. 30, 3025–3035.
Pellegrino, S., Calladine, C.R., 1986. Matrix analysis of statically and kinematically indeterminate frameworks. Int. J. Solids Struct. 22, 409–428.
Skelton, R.E., Pinaud, J.P., Mingori, D.L., 2001. Dynamics of the shell class of tensegrity structures. J. Franklin Inst. 338, 255–320.
Sultan, C., 2013. Stiffness formulations and necessary and sufficient conditions for exponential stability of prestressable structures. Int. J. Solids Struct. 50, 2180–2195.
Sultan, C., Corless, M., Skelton, R.E., 2000. Tensegrity flight simulator. J. Guidance Control Dyn. 23, 1055–1064.
Sultan, C., Corless, M., Skelton, R.E., 2001. The prestressability problem of tensegrity structures: Some analytical solutions. Int. J. Solids Struct. 38, 5223–5252.
Sultan, C., Corless, M., Skelton, R.E., 2002. Symmetrical reconfiguration of tensegrity structures. Int. J. Solids Struct. 39, 2215–2234.
Sultan, C., Skelton, R., 2003. Deployment of tensegrity structures. Int. J. Solids Struct. 40, 4637–4657.
Tanaka, H., Hangai, Y., 1986. Rigid body displacement and stabilization conditions of unstable truss structures. Shells Membr. Space Frames 2, 55–62.
Tibert, A.G., Pellegrino, S., 2011. Review of form-finding methods for tensegrity structures. Int. J. Space Struct. 26, 241–255.
Tran, H.C., Lee, J., 2010. Initial self-stress design of tensegrity grid structures. Comput. Struct. 88, 558–566.
Vassart, N., Motro, R., 1999. Multiparametered formfinding method: application to tensegrity systems. Int. J. Space Struct. 14, 147–154.
Yuan, X.F., Dong, S.L., 2003. Integral feasible prestress of cable domes. Comput. Struct. 81, 2111–2119.
Zhang, J.Y., Guest, S.D., Ohsaki, M., 2009. Symmetric prismatic tensegrity structures: Part I. Configuration and stability. Int. J. Solids Struct. 46, 1–14.